ABSTRACT

The terahertz (THz) region of the electromagnetic spectrum holds promise for spectroscopic imaging of illicit and hazardous materials, and chemical fingerprinting using moment of inertia vibrational transitions. Passive and active devices operating at THz frequencies are currently a challenge, and a promising emerging technology for such devices is optical metamaterials. The very few examples of THz devices based on metamaterials show limited performance and one of the limiting factors is the various losses present in the structures. Reducing dielectric losses in THz metamaterials would allow for improved terahertz devices that can then be used in some of these applications. In addition, there is an interest in fabricating 3D metamaterials, which is a challenge at these and shorter wavelengths due to fabrication constraints. In order to address both of these problems, we have developed a process to fabricate THz metamaterials on free-standing, 1 micron thick silicon nitride membranes. We will present THz transmission spectra and the corresponding simulation results for these metamaterials, comparing their performance with previously fabricated metamaterials on various thick substrates. Finally, we will present a scheme for implementing a 3D THz metamaterial based on stacking and possibly liftoff of these silicon nitride membranes.

INTRODUCTION

Metamaterials are artificial materials formed of an array of subwavelength (~ $\lambda/10$) metallic resonators within or on a dielectric or semiconducting substrate. They exhibit electromagnetic properties not readily available in naturally occurring materials [1-3], the most notable being negative index of refraction. In addition their response is scalable from radio [4] to optical frequencies [5]. Therefore, they have the potential to provide a scale-invariant design paradigm to create functional materials which can enhance our ability to manipulate, control, and detect electromagnetic radiation. The recent growth in the field of metamaterials is partly due to the promise of new devices that exploit these novel electromagnetic properties in all frequency ranges, including terahertz (1 THz ~ 300 μm) [6, 7]. Some of these devices require the fabrication of three-dimensional metamaterials; by stacking individual layers, by creating arbitrarily curved surfaces, or a combination of both [2].

We have developed a process to fabricate THz metamaterials on large area, free-standing thin silicon nitride (Si_3N_4) membranes. Fabricating metamaterials on thin membranes reduces any dielectric losses due to the substrate and enables the implementation of various planar layering schemes. In addition, it allows us to release the membranes and wrap them over curved surfaces, therefore showing a clear path towards creating arbitrarily curved 3D metamaterials.

EXPERIMENT

Fabrication

The metamaterials were fabricated on 550 μm thick 4” silicon (Si) wafers PECVD coated with 1 μm of Si_3N_4. Since PECVD coats all sides of the wafer, the first processing step is to remove the Si_3N_4 from the back in four ~ (3.2 x 2.4) cm^2 areas which will be used to open windows to the metamaterials on the front side, figure 1a), left column. The windows were defined in JSR 5740 photoresist (PR) using standard photolithography before etching the Si_3N_4 using reactive ion

etching (RIE) in a CF4 (40 sccm) and O_2 (10 sccm) atmosphere at 100 mTorr with a power of 100 W for 30 min. Once the Si_3N_4 is removed from the windows on the back side, the wafer was

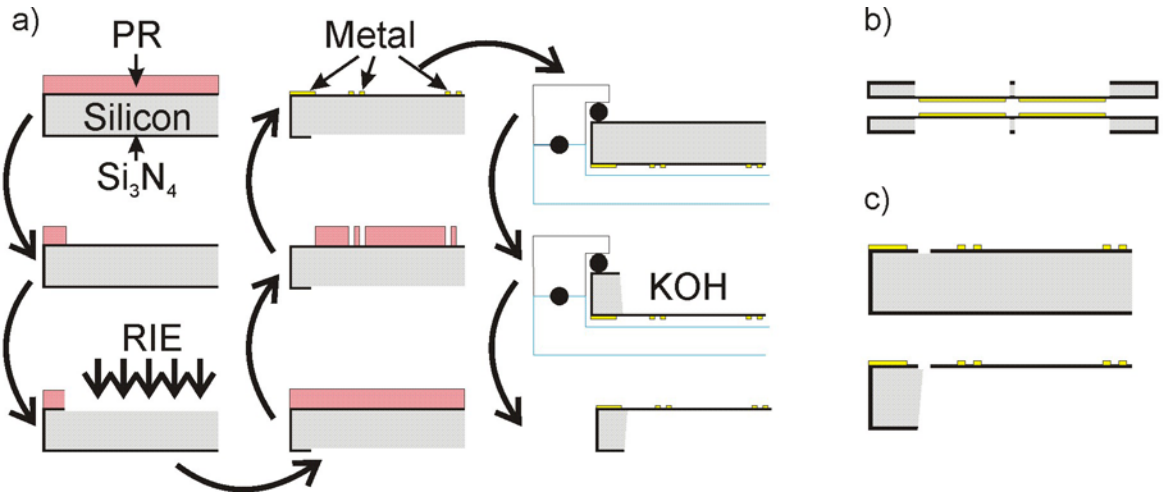

Figure 1. Schematic diagrams of a) the processing steps required to fabricate metamaterials on silicon nitride membranes, b) bilayer stacking and c) chemical liftoff process.

flipped over and the metamaterials were patterned in AZ 5214 PR before evaporating 200Å of Ti followed by 500Å of Au, figure 1a), middle column. After liftoff the wafer was flipped over once more and mounted into a commercial wafer holder from AMMT GmbH that protects the front side during the next step, figure 1a), right column. A KOH bath at 30% dilution for 6 – 8 h at 80 C selectively removes the Si substrate in the Si_3N_4–free window areas defined on the back side in the first process and stops at the Si_3N_4. When removed from the wafer holder, the metamaterials are patterned onto four large-area, free-standing, thin Si_3N_4 windows, see figure 2. Each window has four different metamaterial designs, each covering a ~ (1.3 X 1) cm^2 area. One section in one window is intentionally left blank in order to use as a reference.

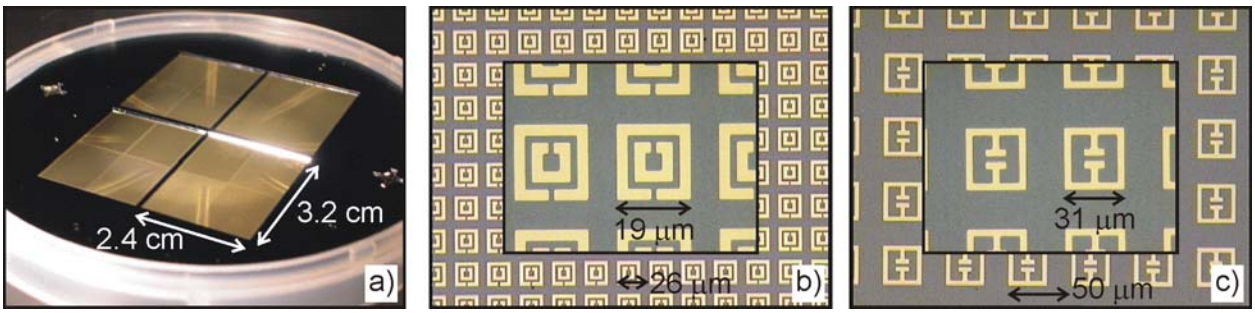

Figure 2. a) Fully processed wafer with the four Si_3N_4 windows evident, b) double Split-Ring Resonator (dSRR) array and b) Electric resonator (E2) array.

Characterization of planar metamaterials on Si_3N_4 membranes

In order to compare the effect of having a thin (1 μm) Si_3N_4 membrane with a thick substrate (hundreds of microns) as substrates or THz metamaterials, we characterized the

electromagnetic response of all 15 metamaterials with a terahertz time-domain spectroscopy (THz-TDS) system. The THz-TDS system is based on photolithographically defined photoconductive antennas for both the source and the detector and has been detailed elsewhere [8]. The experiments were performed at room temperature in a dry air atmosphere (<1% humidity). The THz beam diameter is ~ 3 mm and is easily contained within the sections covered by a particular metamaterial design. The time-varying electric field of the THz transmitted light through the unpatterned section of the Si_3N_4 membrane and through the metamaterial samples were recorded and, after a numerical Fourier transformation, we obtained the THz transmission spectra and the phase change relative to the reference. In all cases the THz radiation was polarized perpendicular to the gaps and transmitted normally through the plane of the metamaterials, see figure 3.

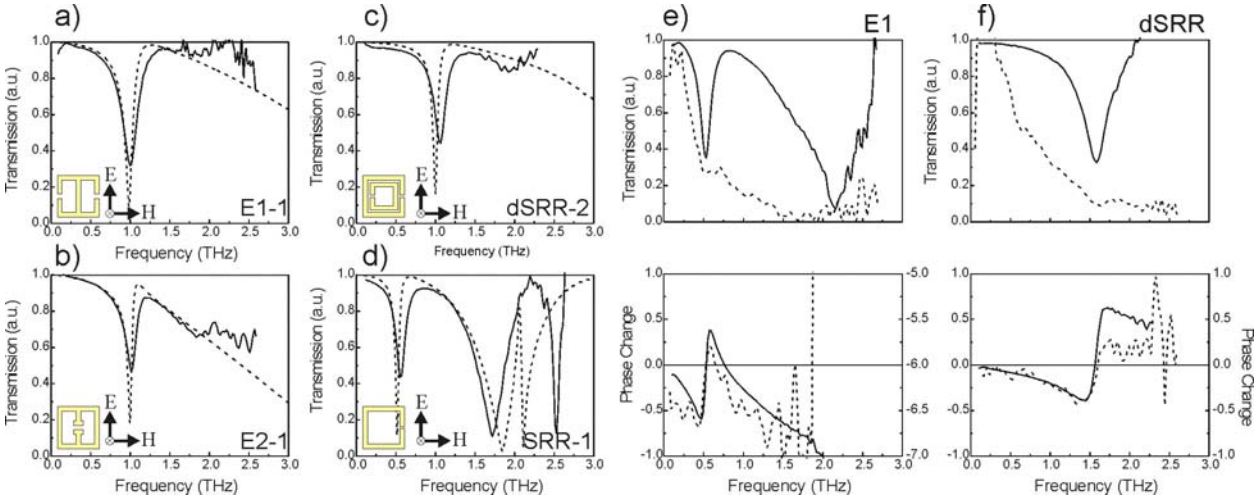

Figure 3. Transmission spectra (solid) and simulation results (dash) for a) E1, b) E2, c) dSRR and d) SRR on planar membranes. Labels refer to designs indicated in Table I. Transmission spectra and phase change for e) E1 and f) dSRR on planar (solid) and curved (dash) membranes.

We also performed electromagnetic modeling using finite-element software [9]. A constant dielectric permittivity of $\varepsilon_{Si_3N_4} = 7$ was used in the simulations. For the metal's response a Drude model was used, where using only Au instead of Ti/Au gave nominally the same results. Figure 3 a) – d) shows the transmission spectra and simulation results for 4 representative metamaterial designs. In most cases we were able to reproduce qualitatively the features observed in the transmission measurements and their relative positions.

Table I lists the geometrical parameters and quality factors (Q) of some of the resonators fabricated on thin Si_3N_4 membranes (in bold) as well as physically similar ones found in the literature fabricated on thick substrates. For all low-frequency resonances, we calculated Q as:

$$Q = \frac{\omega_0}{\Delta\omega}, \tag{1}$$

where ω_0 is the resonant frequency and $\Delta\omega$ is the full width at half maximum. The geometrical parameters are **g** – gap, **w** – metal linewidth, **s** – separation between rings (dSRR) or capacitor plate width (E2), **l** – outer dimension, **p** – lattice constant.

Table I. Geometrical parameters and quality factors. All lengths are in μm.

Design	Ref.	g	w	s	l	p	Substrate	Thickness	Metal	Thickness	*Q*
E1	10	2	4		36	50	SI GaAs	670 μm	Ti/Au	210 nm	6.0
E1-1		2	4		36	50	Si_3N_4	1 μm	Ti/Au	70 nm	**4.5**
E2	10	2	4		36	50	SI GaAs	670 μm	Ti/Au	210 nm	7.0
E2-1		2	4	18	38	50	Si_3N_4	1 μm	Ti/Au	70 nm	**6.4**
dSRR	11	2	6	3	36	50	Silicon	640 μm	Al	200 nm	7.6
	11	2	6	3	36	50	Quartz	1.03 mm	Al	200 nm	8.0
dSRR-1		2	6	3	38	52	Si_3N_4	1 μm	Ti/Au	70 nm	**7.3**
	12	4	4	3	30	44	Quartz	0.8 mm	Cu	320 nm	6.3
dSRR-2		2	4	4	29	46	Si_3N_4	1 μm	Ti/Au	70 nm	**6.3**
SRR	7	2	6		36	50	HR GaAs	670 μm	Cu	3 μm	6.2
SRR-1		2	4		55	75	Si_3N_4	1 μm	Ti/Au	70 nm	**4.4**

The first 7 samples where chosen because the geometrical parameters of our samples and those found in the literature are very similar. The last 4 were chosen on the basis of having very similar low-frequency resonance positions (0.9 THz dSRR in [12] and 0.5 THz SRR in [7], see Fig. 3).

Three-dimensional implementations and characterization

Our first approach to implement 3D metamaterial using thin Si_3N_4 membranes is to fabricate two wafers with the same metamaterial patterns and stacking them with the metamaterials facing each other, figure 1b). This opens up the possibility of studying the metamaterial properties as a function of separation between the layers, registry between the units and relative orientation of the units [13, 14]. To avoid artifacts in the measurements, the wafers must be kept parallel by introducing a spacer of a known thickness around the edges.

Another approach is to remove the patterned membrane from the Si wafer after fabrication. To accomplish this, one can place the wafer front side down onto a stack of lens cleaning paper and, with a sharp razor blade, cut out the Si_3N_4 window. Using tweezers one can move the membrane onto a host material which can be planar, such as a piece of mylar of a known thickness for the stacking scheme, or a 3D object such as a Teflon tube (mylar and Teflon® PTFE are transparent at THz frequencies). Figure 4 shows two different instances of a curved metamaterial fabricated in this manner.

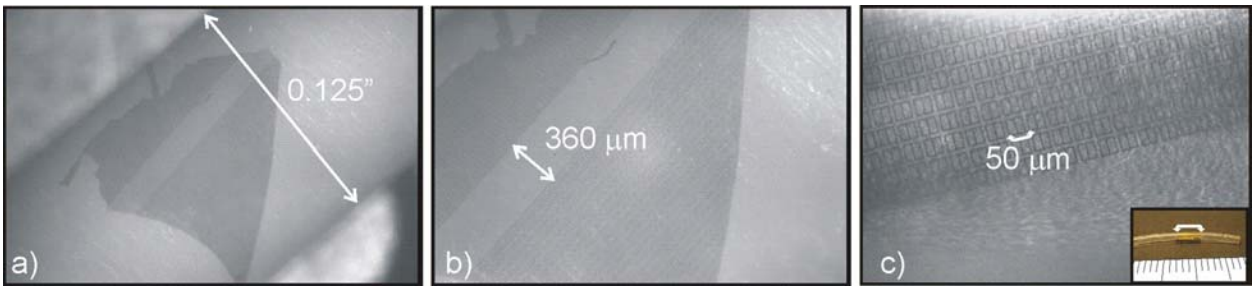

Figure 4. Microscope images of a piece of metamaterial covered, Si_3N_4 membrane, wrapped around a) and b) a Teflon tube and c) a 1.5 mm diameter tubing. Scale of inset mm.

Figures 3 e) and f) illustrate the frequency-dependent amplitude transmission and the phase change of two different metamaterial designs wrapped around a Teflon tube. The reference was a bare piece of Teflon tube. For comparison, they are plotted with the corresponding planar metamaterial covered membrane's response. In both curved metamaterials we observe a small decrease in transmission close to the resonance of the planar metamaterials on top of a uniformly decreasing background. The phase change data clearly confirms this observation.

DISCUSSION

Fabrication of THz metamaterials on 1 μm thick Si_3N_4 membranes was implemented with the goal of reducing dielectric losses from the substrate and developing pathways towards 3D metamaterial structures. We successfully modeled, fabricated and characterized them. The observed differences between measurements and simulations might be related to having used a constant dielectric permittivity in the simulations in place of a frequency dependent permittivity which was not available in the THz region. The case in which the modeling differed the most from the experiments was for the higher frequency resonances in SRR-1 (figure 3d). This might be due to the effect of higher-order modes [15] but it is still under investigation.

All of the structures fabricated on Si_3N_4 membranes have comparable *Q*'s to similar structures that appear in the literature. This could imply that dielectric losses from the substrate are not as important as previously thought, but one also needs to take into consideration that in our samples the metallization thickness (20 nm Ti/ 50 nm Au) is less than the skin depth (δ) of the THz radiation (at 1 THz, $\delta_{Au} \sim 75$ nm, $\delta_{Ti} \sim 325$ nm), therefore it is not as efficient at screening the field as in other samples in the literature. It is interesting to note that the resonances are better defined than the only other reference in the literature to THz metamaterials on thin silicon nitride membranes [16].

The approach described for layering is currently limited to two layers as the thickness of the Si wafers used (550 μm) is several times larger than the periodicity of the THz metamaterial arrays (at most 80 μm). To extend this stacking scheme to more layers, we can reduce the thickness of the Si wafer, use smaller pieces which can be nested into each other to form a 3D structure or remove the membranes from the substrate. Currently the liftoff procedure for the Si_3N_4 membrane is done manually, therefore it is not well controlled and tearing occurs. To overcome this problem we can define a Si_3N_4–free trench at the edge of the window area covered by the metamaterials on the front side **before** actually patterning the metamaterials. When the wafer is placed in KOH, the membrane will be released, figure 1c).

To our knowledge, this is the first implementation and measurement of a curved metamaterial at THz frequencies. The resonances in transmission can be resolved although riding on top of a currently unexplained, uniformly decreasing background, but are clearly defined in the phase change data. Further studies need to be done to fully understand the response.

CONCLUSIONS

We have successfully fabricated THz metamaterials on large-area, free- standing, thin Si_3N_4 membranes and have demonstrated one scheme for fabricating layered and/or curved metamaterials. The performance of the planar metamaterials on membranes, as judged by the quality factor of the low-frequency resonances, is comparable to those fabricated on thick substrates. A better understanding of dielectric losses, the role of the effective permittivity of the

supporting media and metallization thickness might help improve their response. We successfully characterized the first implementations of curved THz metamaterials and corroborated the location of their resonant response, but there are still many open questions about the details of their response. Metamaterials on thin membranes may prove practical and useful for implementing fully 3D metamaterial structures across the electromagnetic spectrum.

ACKNOWLEDGMENTS

We acknowledge support from the Center for Integrated Nanotechnologies. X. G. P. also acknowledges support from the IC Postdoctoral Fellowship Program. Sandia is a multiprogram laboratory operated by Sandia Corporation, a Lockheed Martin Company, for the United States Department of Energy's National Nuclear Security Administration under Contract DE-AC04-94AL85000.

REFERENCES

1. D. R. Smith, W. J. Padilla, D. C. Vier, S. C. Nemat-Nasser and S. Schultz, *PRL* **84**, 4184 (2000).
2. R. A. Shelby, D. R. Smith and S. Schultz, *Science* **292**, 77 (2001).
3. J. B. Pendry, A. J. Holden, D. J. Robbins and W. J. Stewart, *IEEE Trans. Microwave Theory Tech.* **47**, 2075 (1999).
4. M. C. K. Witshire, J. B. Pendry, I. R. Young, D. J. Larkman, D. J. Gilderdale,and J. V. Hajnal, *Science 291*, 849 (2001).
5. C. Enkrich, M. Wegener, S. Linden, S. Burger, L. Zschiedrich, F.Schmidt, J. F. Zhou, Th. Koschny, and C. M. Soukoulis, *PRL* **95**, 203901 (2005).
6. B. Ferguson and X-C Zhang, *Nature Materials* **1**, 26 (2002).
7. W. J. Padilla, A. J. Taylor, C. Highstrete, M. Lee and R. D. Averitt, *PRL* **96**, 107401 (2006).
8. J. F. O'Hara, J. M. O. Zide, A. C. Gossard, A. J. Taylor and R. D. Averitt, **APL 88**, 25, 251119 (2006).
9. CST Microwave Studio ®, © 2005 CST – Computer Simulation Technology, Wellesley Hills, MA, USA. www.cst.com
10. W. J. Padilla, M. T. Aronsson, C. Highstrete, M. Lee, A. J. Taylor and R. D. Averitt, *PRB* **75**, 041102R (2007).
11. A. K. Azad, J. Dai and W. Zhang, *Opt. Lett.* **31**, 5, 634 (2006).
12. X.-L. Xu, B.-G. Quan, C.-Z. Gu and L. Wang, *J. Opt. Soc. Am. B* **23**, 6, 1174 (2006).
13. P. Gay-Balmaz and O. J. F. Martin, *J. Appl. Phys.* **92**, 2929 (2002).
14. N. Katsarakis, G. Konstantinidis, A. Kostopoulos, R. S. Penciu, T. F. Gundogdu, M. Kafesaki, E. N. Economou, Th. Koschny and C. M. Soukoulis, *Opt. Lett.* **30**, 1348 (2005).
15. J. F. O'Hara, E. Smirnova, H.-T. Chen, A. J. Taylor, R. D. Averitt, C. Highstrete, M. Lee and W. J. Padilla, *J. Nanoeleco. Optoelectron.* **2**, 90 (2007).
16. M. C. Martin, Z. Hao, A. Liddle, E. H. Anderson, W. J. Padilla, D. Schurig and D. R. Smith, *Conference Proceedings of IEEE IRMMW-THz 2005*, vol. **1**, 34 – 35 (2005).